

## A new technique to calculate the electronic structure of two-dimensional disordered systems

This article has been downloaded from IOPscience. Please scroll down to see the full text article.

1997 J. Phys.: Condens. Matter 9 981

(<http://iopscience.iop.org/0953-8984/9/5/005>)

View [the table of contents for this issue](#), or go to the [journal homepage](#) for more

Download details:

IP Address: 171.66.16.207

The article was downloaded on 14/05/2010 at 06:14

Please note that [terms and conditions apply](#).

# A new technique to calculate the electronic structure of two-dimensional disordered systems

A K Yildiz<sup>†‡</sup> and J L Beeby<sup>‡</sup>

<sup>†</sup> University of Firat, Faculty of Science, Department of Physics, 23169 Elazig, Turkey

<sup>‡</sup> University of Leicester, Department of Physics and Astronomy, Leicester LE1 RH7, UK

Received 11 September 1996, in final form 25 October 1996

**Abstract.** The purpose of this work is to investigate the electronic structure of two-dimensional structurally disordered solids by means of a method based on multiple-scattering theory. The theoretical technique is applied to some two-dimensional models which can be varied from the limit of a perfect to a completely disordered structure. The models are continuous structural networks with different-fold coordinations of atoms in planar structures. The spectral density is determined through a self-consistent approach. Using the spectral density, the convergence of the technique is analysed through calculations of the density of electronic states, and the variation of the density of electronic states with respect to varying disorder in the structure is determined. In particular, the convergence of the technique for the calculation of the density of electronic states as a function of the size of the matrix representation used is confirmed and it is shown that the degree of disorder in two-dimensional systems significantly influences the density of electronic states.

## 1. Introduction

Although significant progress has been made in both theoretical and experimental aspects of disordered systems, many problems remain [1–7]. Progress in the study of these systems, in particular structurally disordered systems, has been relatively slow and delayed in comparison with that of ordered (crystalline) materials. Two principal reasons for this delay are the complexity of the mathematical problems naturally arising in the study of such systems [8]. In part, the increasing interest in disordered systems reflects the continuing growth in the technological importance of materials such as alloys, amorphous semiconductors, liquid metals, and glasses and their application in photovoltaic cells, thin-film devices, and so on.

For disordered systems, the conventional concepts (Bloch's theorem, quasi-momentum  $k$ , unit cell, Brillouin zone, symmetry, and wave numbers) are no longer valid, and familiar constructs such as the dispersion relation are no longer defined. Because there is such a difference between excitations in ordered and disordered systems one finds that methods which have proved quite adequate for ordered crystals generally yield little information on disordered systems. For this reason, a variety of new methods have inevitably been devised and used. One example is the development of sophisticated perturbation techniques in many-body theory, in particular the use of Green functions and the total scattering matrix.

In this paper we shall consider only the density of electronic states (DOS). The manifestation of disorder in the electronic states can appear in various forms: states may

occur inside the band gaps of the ordered system [9], bands broaden as the band edges shift, singularities smear out if there is no long-range order, and tails may appear in the DOS. It is also clear that short-range order (SRO) plays an important role in determining the DOS, e.g. fluctuations in SRO, such as bond angle distortions, lead to tailing of states into the gap at the band edges. The coherent potential approximation has not proved effective for structural disorder, and it is desirable to have an approach which does not depend on finite boundary conditions.

In this work we shall investigate the behaviour of two-dimensional disordered systems based on some simple models. Two-dimensional systems can be realized in layered compounds, such as graphite intercalation compounds, in which the atomic layers are widely separated and weakly interacting. In experimental studies, the inversion layers used in the quantized Hall effect provide an example of two-dimensional systems important in technology as do metal-oxide–semiconductor space charge layers and semiconductor heterostructures [10, 11].

We shall calculate the DOS for different two-dimensional structurally disordered models, for example with various numbers of near neighbours. The calculation is based on a method due to Beeby and Hayes [12] which uses multiple-scattering theory and can be used to calculate the electronic structure of any disordered system. Since the technique is new in application to two-dimensional disordered systems, the reliability of the method will first be demonstrated by considering its convergence. Then the variation of the DOS with varying structural disorder will be calculated for some well known two-dimensional models. This work also serves to underpin the three-dimensional studies [12–14], for which it is difficult to explore convergence properties.

In section 2 the formal theory underlying the calculations will be outlined and the essential equations given specifically for the case of two-dimensional systems. This is extended and illustrated in section 3 with the introduction of a suitable notation for describing the disorder. It is shown in section 4 how the problem may be reduced to a numerically tractable form. In section 5 a suitable model potential is introduced and numerical procedures developed. The DOS calculations are then presented in section 6, demonstrating that the method converges and that useful results can be obtained. The paper ends with a brief discussion.

## 2. The formal theory

The BH method, based on multiple-scattering theory for non-overlapping muffin-tin potentials, will be outlined in this section. It was applied [13, 14] to tetrahedrally bonded disordered systems in three dimensions, which has given confidence for application to other systems, in particular, for systems which possess short-range order (SRO).

The mathematical procedures of multiple-scattering theory for two-dimensional disordered systems were developed in [15] and follow those for three dimensions [16]. The DOS can be calculated from the imaginary part of the total scattering matrix as the integral over energy of the spectral density [16],

$$\rho(\mathbf{k}, E) = -(\pi \Omega_0)^{-1} (E - k^2)^{-2} \text{Im}\langle \mathbf{T}(\mathbf{k}) \rangle \quad (1)$$

where  $E$  is the electron energy,  $\mathbf{k}$  is the electron momentum, and  $\Omega_0$  is the volume of the system. The average in this equation is over a suitable statistical ensemble which represents the disordered system.  $\mathbf{T}(\mathbf{k})$ , the total scattering matrix, can be expanded for a

two-dimensional disordered system in the series

$$\begin{aligned} \mathbf{T}(\mathbf{k}) = & 2\pi \sum_{mm'} (-i)^{m-m'} \exp[i(m-m')\theta_k] \{ \mathbf{t}(k, k) + \sum_{b(\neq a)} \mathbf{t}(k, \kappa) \mathbf{G}^{ab}(\kappa, k) \mathbf{t}(k, k) \\ & + \sum_{b(\neq a), c(\neq b)} \mathbf{t}(k, \kappa) \mathbf{G}^{ab}(\kappa, k) \mathbf{t}(\kappa, \kappa) \mathbf{G}^{bc}(\kappa, k) \mathbf{t}(\kappa, k) + \dots \}_{mm'} \end{aligned} \quad (2)$$

where  $\kappa = E^{1/2}$ , and the elements of each  $\mathbf{t}$  and  $\mathbf{G}$  are matrices labelled by angular momentum indices  $m$  and  $m'$ . The  $t$ -matrix transforms are defined by

$$t_{mm'}(p, p') = \frac{1}{2\pi} \int J_m(pr) e^{-im\theta_r} t(\mathbf{r}, \mathbf{r}') J_{m'}(p'r') e^{-im'\theta_{r'}} d\mathbf{r} d\mathbf{r}'. \quad (3)$$

If the potential is circularly symmetric,  $\mathbf{t}_{mm'} = \mathbf{t}_m \delta_{mm'}$ , and so  $\mathbf{t}$  is diagonal in angular momentum. The elements of the matrix  $\mathbf{G}$  can be shown to be [15]

$$G_{mm'}^{ab} = - \sum (-i)^{m'-m+v} J_v(\mu R) K_{m'-m}(\mu R) e^{i(m'-m-v)\theta_R} e^{iv\theta_k}. \quad (4)$$

We shall confine ourselves to the energy range  $E < 0$  for which  $\mu = (-E)^{1/2}$  is real.  $R$  is the distance between the two atoms and the bond direction is denoted by  $\theta_R$ . Then

$$\begin{aligned} \text{Im}(\mathbf{T}(\mathbf{k})) = & 2\pi \text{Im} \sum (-i)^{m-m'} \exp[i(m-m')\theta_k] [t_m(k, i\mu) / t_m(i\mu, i\mu)] \\ & \times \left\langle \sum_a \mathbf{F}^a(i\mu, k) \right\rangle_{mm'} t_{m'}(i\mu, i\mu) [t_{m'}(i\mu, k) / t_{m'}(i\mu, i\mu)] \end{aligned} \quad (5)$$

where  $\mathbf{F}^a$  contains all those multiple-atom scattering paths in which the electron starts at atom  $a$  and is defined by [12]

$$\mathbf{F}^a = \mathbf{1} + \sum \mathbf{tG}^{ab} + \sum \mathbf{tG}^{ab}\mathbf{tG}^{bc} + \dots = \mathbf{1} + \sum \mathbf{tG}^{ab}\mathbf{F}^b. \quad (6)$$

$\mathbf{F}^a$  depends implicitly on the positions of all the neighbouring atoms and modifies the free electron propagator to take into account all scattering sequences. These defining equations will be applied in the next section to the specific physical systems of interest.

### 3. Application to two-dimensional disordered systems

To demonstrate the application of the technique to two-dimensional disordered systems, we shall begin by defining the self-consistent function  $\mathbf{F}^a$  given by equation (6) for a general model in terms of some variables describing each atomic environment. The averages over the disordered structures will then be performed for this model and the resultant matrix equations solved to give calculated DOS.

We illustrate the procedure initially by using a continuous structural network with threefold coordination of atoms in a planar structure related to the honeycomb lattice, and the bond lengths between two atoms being treated as always the same. This corresponds to neglecting variations in the motion of electrons between pairs of atoms, often referred to as hopping. The disorder manifests itself in the bond angles, giving a structure with rings of various sizes. The disorder in such a system can be described in a statistical way by defining a distribution function on the bond angles which approximates the discrete distribution of bond angles arising from the actual ring statistics. To describe each atom and its environment, we define a set of coordinate axes in which the associated atomic environment has some orientation specified by angles. The propagator modifier  $\mathbf{F}$  can then be written as a function of all the angles required to specify the system. However in more complicated structurally disordered models the variable parameters could be extended by including other variables such as bond lengths or the number and species of neighbours.

The local axis that we have chosen for atom *a*, illustrated in figure 1, is directed to a nearest-neighbour atom *b* in the *xy* plane. The deviation of this local axis from the coordinate axis is labelled  $\theta_a$  on the model. We assume that the first scattering is taking place at atom (or ion) *a*, and after scattering there the electron may propagate to a nearest neighbour atom, such as atom *b*, and scatter there. This sequence of scattering goes on throughout the system as specified by equation (6). The contribution to the density of states of these sequences from atom *a* depends on the positions of the other potentials, such as the atom *b*, relative to *a*, and the dominant part for  $E < 0$  is related to the nearest-neighbour atoms. Therefore, for a particular atom, the function  $\mathbf{F}$  can be approximately described by treating it as a function only of its local set of angles. Averaging over the spread of distant angles but keeping the local angles fixed, the scattering function corresponding to atom *a* can be written in terms of its near neighbour, atom *b*, as

$$\langle \mathbf{F}^a \rangle_a = \mathbf{1} + \sum \mathbf{t} \langle \mathbf{G}^{ab} \mathbf{F}^b \rangle_a \quad (7)$$

where the subscript *a* on the averages indicates that the angles at *a* are fixed. Note that this implies that the positions of the nearest neighbours, *b*, of *a* are fixed.

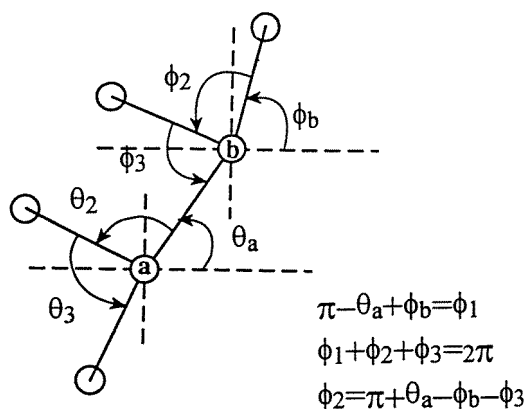


Figure 1. A simple model with threefold coordinated structure.

We shall approximate each  $\mathbf{F}^a$  by a Fourier series involving the local angles only so that

$$\mathbf{F}^a(\theta_a, \theta_2, \theta_3) = \sum_{m_i=-\infty}^{\infty} \mathbf{A}_m e^{(im_1\theta_a + im_2\theta_2 + im_3\theta_3)} \quad (8)$$

and

$$\mathbf{F}^a(\phi_b, \phi_2, \phi_3) = \sum_{m'_i=-\infty}^{\infty} \mathbf{A}_m e^{(im'_1\phi_b + im'_2\phi_2 + im'_3\phi_3)} \quad (9)$$

using the notation of figure 1. The subscript  $m$  on  $\mathbf{A}$  represents the vector  $(m_1, m_2, m_3)$  and it is essential to note that these angular indices are distinct from those of equations (2)–(5), which are implicit in  $\mathbf{F}$ ,  $\mathbf{A}$ , and  $\mathbf{G}$ . The  $m_i$  are integers i.e.  $0, \pm 1, \pm 2, \dots$ . The propagator  $\mathbf{G}^{ab}$  in equation (7) is given by equation (4) with  $R$  the magnitude of  $\mathbf{R}_b - \mathbf{R}_a$  taken to be the same for all bonds.  $\mathbf{G}^{ab}$  depends only on the nearest-neighbour distribution, which is invariant in equation (7) so  $\mathbf{G}^{ab}$  is outside the structural average. Then the only function

on the right hand-side of equation (7) related to the disorder associated with atom  $a$  is the function  $\mathbf{F}^b$ , which is required to be averaged over the angles  $\phi$ .

To implement the averaging, a probability function  $P(\theta_i)$ , for the angles around atom  $a$ , as in figure 1, can be introduced in terms of some parameters describing the system under consideration. In this work a Gaussian form will be taken,  $P(\theta_i) = N e^{-(\theta_i - 2\pi/n)^2/\omega^2}$ . This function describes the probability of finding a particle  $i$  between  $\theta_i$  and  $\theta_i + d\theta_i$ , where  $N$  is the normalization coefficient,  $n$  is the coordination number (e.g for a triangular lattice  $n = 6$ , square lattice  $n = 4$ ), and  $\omega$  is a parameter representing the degree of disorder.  $\omega$  can be varied from 0.0 to  $\infty$ , i.e from complete order to a circularly symmetric distribution which corresponds to complete disorder.

To average equation (9) one is required to multiply the equation by the probability functions  $P(\phi_i)$ , and to integrate over the angles  $\phi_1, \phi_2$ , etc. This gives

$$\langle \mathbf{F}^b \rangle = \sum \mathbf{A}_m e^{im'_1\theta_b} \Gamma(m'_1, m'_2, \dots; \omega). \quad (10)$$

Here  $\Gamma(m'_1, m'_2, \dots; \omega)$  will be called the structural factor and incorporates the terms related to the rotational angles and disorder parameters. This equation is quite general and becomes, for example, for the model in figure 1, in which  $n = 3$ ,

$$\Gamma(m'_1, m'_2, m'_3; \omega) = e^{-i\pi m'_1} e^{-i2\pi(m'_1+m'_2+m'_3)/3} \\ \times \exp \frac{\omega^2}{4} \left[ \frac{(m'_1 + m'_2 + m'_3)^2}{3} - (m_1'^2 + m_2'^2 + m_3'^2) \right]. \quad (11)$$

Finally, equation (7) becomes

$$\mathbf{A}_{m_1 m_2 m_3} = \delta_{m_1,0} \delta_{m_2,0} \delta_{m_3,0} \mathbf{1} - \sum_{vm'_1 m'_2 m'_3} \mathbf{tG}_{vm''} \mathbf{A}_{m'_1 m'_2 m'_3} \Gamma(m'_1, m'_2, m'_3; \omega) \delta(m'_1 + m'' - v - m_1) \\ \times (\delta_{m_2,0} \delta_{m_3,0} + \delta_{m_1, m_2} \delta_{m_3,0} + \delta_{m_1, m_2} \delta_{m_1, m_3}) \quad (12)$$

where  $G_{vm''} = (-i)^{m''+v} J_v(kR) K_{m''}(\mu R)$  and the two types of index are linked because  $m'' = m' - m$ , as in equation (4). The three terms in the final brackets originate from the three neighbours. Thus the coefficient  $\mathbf{A}$  satisfies a matrix equation and gives  $\mathbf{F}$  through equation (8). Not all of the columns of  $\mathbf{A}_m$  are required because the spectral density is independent of the direction of  $\mathbf{k}$  for a system which has no preferred axis. Therefore, the direction of  $\mathbf{k}$  can be set to the  $x$  direction in the laboratory coordinate frame.

We write equation (12) in matrix form to evaluate its eigenvalues and eigenvectors for calculating the spectral density. Then

$$\mathbf{A} = \mathbf{e} + \mathbf{MA} \quad (13)$$

where  $\mathbf{A}$  can be visualized as a column vector and each element of the column is labelled by indices  $m_1, m_2, m_3$  from the expansion introduced in equation (8). All the quantities in equation (13) have elements which are matrices. For convenience the indices are dropped and the structural factors are incorporated in the matrix  $\mathbf{M}$ .  $\mathbf{M}$  is a complex (through  $\mathbf{G}$ ) and asymmetric matrix with analogous indices expressing the coupling among the elements of  $\mathbf{A}$ . Physically its eigenvalues must be real and this can be confirmed computationally. It will be shown in the next section that it is possible to transform  $\mathbf{M}$  to a symmetric real matrix. The solution of equation (13) can be found in terms of the eigenvalues,  $\lambda_i$ , and left and right eigenvectors,  $\mathbf{u}_i^T$  and  $\mathbf{u}_i$ , of  $\mathbf{M}$ :

$$\mathbf{A} = \sum_i \mathbf{u}_i (1 - \lambda_i)^{-1} \mathbf{u}_i^T \cdot \mathbf{e} \quad (14)$$

where  $e$  is a column vector with elements which are equal to one when  $\mathbf{m} = \mathbf{0}$  and zero otherwise.  $\rho(\mathbf{k}, E)$  depends on the imaginary part of  $\mathbf{A}_{000}$  and is non-zero only for values of  $\mathbf{k}$  and  $E$  such that  $\lambda_i = 1$ , giving

$$\int \rho(\mathbf{k}, E) d\theta_k = -\frac{1}{\pi} \frac{1}{(E - k^2)^2} \sum_{mm'} \left[ \frac{s_m(k)}{s_m(i\mu)} \right] \left[ \frac{s_{m'}(k)}{s_{m'}(i\mu)} \right] \frac{s_m(i\mu)}{\pi/2} \text{Im}[\mathbf{A}_{000}]_{mm'} \quad (15)$$

where

$$\text{Im} \mathbf{A}_{000} = -\pi \sum_i [\mathbf{u}_i]_{000} \delta(E - E_i(k)) (\partial \lambda_i / \partial E)^{-1} (\mathbf{u}_i^T \cdot \mathbf{e}). \quad (16)$$

The function  $s$  is related to the scattering potential and must be derived from the chosen potential. This will be discussed in section 5. Before proceeding with such a calculation, the matrix equation (12) needs to be put into a more readily solvable form, symmetric form.

#### 4. Matrix reduction to computable and symmetric form

In this section we shall transform equation (12) into a computable and symmetric form before solving it numerically. To do this let us define a new vector by

$$\Lambda_{m_1} = \sum_{m_2 m_3} \Gamma(m_1, m_2, m_3; \omega) \mathbf{A}_{m_1, m_2, m_3}. \quad (17)$$

This then satisfies the equation

$$\Lambda_{m_1} = \delta_{m_1, 0} \mathbf{1} - \gamma_{m_1} \mathbf{t} \sum_{vm''m'_1} G_{vm''} (-)^{m'_1} \delta(m'_1 + m'' - v - m_1) \Lambda_{m'_1} \quad (18)$$

where

$$\gamma_{m_1} = \Gamma(m_1, 0, 0; \omega) + \Gamma(m_1, m_1, 0; \omega) + \Gamma(m_1, m_1, m_1; \omega) \quad (19)$$

is real and positive. Once  $\Lambda$  is formed the values of  $\mathbf{A}$  can be recovered using equations (17) and (12). In order to make the matrix on the right-hand side symmetric a further transformation

$$\Omega_{m_1} = (-i)^{m_1+m} \Lambda_{m_1} / (\gamma_{m_1} / \gamma_0)^{1/2} \quad (20)$$

gives

$$\Omega_{m_1} = \delta_{m_1, 0} \mathbf{1} - \mathbf{t} \gamma_{m_1}^{1/2} \sum_{m'_1, m''} (-i)^{m''} J_{m'_1+m''-m_1}(kR) K_{m''}(\mu R) (-) \gamma_{m'_1}^{1/2} \Omega_{m'_1} \quad (21)$$

where the matrix is Hermitian if  $m'' \neq 0$  but becomes real if only the s-wave case,  $m = m' = 0$ , is considered. The imaginary part of  $\mathbf{A}_{000}$  from (12) and (17) is just  $\text{Im} \Lambda_0 / \gamma_0$  and so becomes  $\text{Im} \Omega_0 (-i)^m / \gamma_0$  using (20). The required result, replacing (15), is of exactly the same form but the eigenvalues and eigenvectors now refer to the symmetric matrix on the right-hand side of (21).

#### 5. Density of states calculations for different structures

In this section the numerical procedures just described will be applied to some specific examples. A circularly symmetric potential will be used and it will be assumed that only s-wave scattering is significant. In the general case, as has been noted earlier,  $\mathbf{t}$  and the coefficients  $\mathbf{G}$ , and hence  $\mathbf{A}$ , are all matrices in the angular momentum representation. For a circularly symmetric potential the matrix  $\mathbf{t}$  is diagonal in angular momentum, but  $\mathbf{G}$  is

not, describing propagation from one atom site to another and giving rise to effects such as s-p hybridization. By considering only s-wave scattering only those terms for which  $m, m' = (0, 0)$  arise. Thus the expression for  $G_{vm''}$  in equation (1) becomes

$$G_{vm''} = -(-i)^v J_v(kR) K_0(\mu R) \delta_{m'',0}. \quad (22)$$

Hence the momentum dependence of the matrix is due to  $J_{m'_1-m_1}(kR)$  and the energy dependence takes the form

$$U(E) = t_0(i\mu, i\mu) K_0(\mu R). \quad (23)$$

Finally, we have a matrix equation for the vector  $\Omega$ , which is now a simple vector;

$$\begin{aligned} \Omega_{m_1} &= \delta_{m_1,0} - t_0 \sum_{m'_1} \sqrt{\gamma_{m_1}} \sqrt{\gamma_{m'_1}} J_{m'_1-m_1}(kR) K_0(\mu R) (-)^{m'_1} \Omega_{m'_1} \\ &= \delta_{m_1,0} + U(E) \sum_{m_1} H_{m_1,m_1'}(k) \Omega_{m_1'}. \end{aligned} \quad (24)$$

This is the general expression that we shall use to evaluate the eigenvalues and eigenvectors, from which we will find the electronic band structure and calculate the DOS.

Before presenting the detailed results it is useful to consider the approximation of taking the circularly symmetric average, i.e  $\omega$  large in  $P(\Theta_i)$ , which means that we retain only the term  $v = 0$ . Then equation (24) has the solution

$$\Omega_0 = (1 - U(E) H_{00}(k))^{-1}. \quad (25)$$

Taking the case of  $n = 3$ ,  $\gamma_{m_1'} = 2 \cos(2m_1'\pi/3) e^{-\omega^2 m_1'^2/6} + 1$ ,  $\gamma_0 = 3$  and  $H_{00} = -3J_0(kR)$ . The imaginary part of the solution is then

$$\text{Im} \Omega_0 = -\pi \delta(E - E(k)) H(k) (\partial U / \partial E)^{-1}. \quad (26)$$

For a narrow s band and  $E \ll 0$  the energy dependence is given by  $U(E) \cong W/(E - E_b)$  [12], where  $E_b$  is the bound state energy of a single muffin-tin potential and  $W$  is a parameter related to the band width. The general limits on the band can simply be found from a perfect hexagonal lattice or the so-called honeycomb lattice for which  $n = 3$ . It is known in general that the energy in the tight-binding approximation is given as  $E_k \cong E_0 \pm W |\sum e^{ik \cdot R}|$ , which can be expanded in a power series near  $k = 0$  and from which the band width can be predicted. The bottom of the band is near  $k = 0$  with energy  $E \cong E_0 - 3W$ . The top of the band occurs near the corners of the Brillion zone (BZ) with energy  $E \cong E_0 + 3W$ .

When an explicit potential is used, the functions  $s(k)$  and  $s(i\mu)$  used in equation (15) must be evaluated. An example of this calculation will now be presented. We shall consider a square well potential of circular form and radius  $r_{sw}$ . Because of the muffin-tin requirement  $r_{sw} \leq R/2$ . Thus  $v(r) = V_{sw} < 0$  for  $r < r_{sw}$  and  $v(r) = 0$  if  $r > r_{sw}$ . The radial solution of the Schrödinger equation for a two-dimensional potential can be written as

$$R_0(r) = B J_0(\xi r) \quad r < r_{sw} \quad (27a)$$

and

$$R_0(r) = C J_0(i\mu r) + D Y_0(i\mu r) \quad r > r_{sw} \quad (27b)$$

where  $\xi = \sqrt{-(E - V_{sw})}$  and  $\mu = \sqrt{-E}$ . The energy range of interest is  $V_{sw} < E < 0$  so that both  $\xi$  and  $\mu$  are real. For convenience we have taken  $\hbar^2/2m = 1$ .  $Y_n(z)$  is a Bessel function of the second kind (or Weber's function). In addition to these two equations, the radial wave function can also be defined in a different form as in [15] and [16]. When integrated, this equation yields for  $r > r_{sw}$

$$s_0(r)/V_{sw}(r) = -(\pi/2) I_0(\mu r) - K_0(\mu r) s_0(i\mu) \quad (28)$$



where  $I_0(\mu r)$  and  $K_0(\mu r)$  are modified Bessel functions [17]. Since  $R_0(r) \propto s_m(r)/V_{sw}(r)$ , one can obtain the coefficients  $B$ ,  $C$ , and  $D$  by using the boundary conditions, giving

$$\begin{aligned} B &= -(\pi/2)[I_0(\mu r_{sw}) + (2/\pi)s_0(i\mu)K_0(\mu r_{sw})] \\ C &= -(\pi/2)[1 + is_0(i\mu)] \\ D &= (\pi/2)s_0(i\mu). \end{aligned} \quad (29)$$

Hence, using these coefficients,  $s_0(r)$  for  $r < r_{sw}$  is

$$s_0(r) = -(\pi/2)V_{sw}[[I_0(\mu r_{sw}) + (2/\pi)s_0(i\mu)K_0(\mu r_{sw})]/J_0(\xi r_{sw})]J_0(\xi r). \quad (30)$$

The functions  $s_0(i\mu)$  and  $s_0(k)$  are then

$$\begin{aligned} s_0(i\mu) &= (\pi/2)r_{sw}I_0(\mu r_{sw})[\mu I_1(\mu r_{sw})J_0(\xi r_{sw}) + \xi J_1(\xi r_{sw})I_0(\mu r_{sw})]/\{J_0(\xi r_{sw}) \\ &\quad - r_{sw}K_0(\mu r_{sw})[\mu I_1(\mu r_{sw})J_0(\xi r_{sw}) + \xi J_1(\xi r_{sw})I_0(\mu r_{sw})]\} \end{aligned} \quad (31)$$

and

$$s_0(k) = \frac{V_{sw}Br_{sw}}{k^2 - \xi^2} [kJ_1(kr_{sw})J_0(\xi r_{sw}) - \xi J_1(\xi r_{sw})J_0(kr_{sw})]. \quad (32)$$

Finally, the relation between  $s_0(i\mu)$  and  $s_0(k)$  can be given as

$$\frac{s_0(k)}{s_0(i\mu)} = \frac{V_{sw}}{k^2 - \xi^2} \left[ \frac{kJ_1(kr_{sw})J_0(\xi r_{sw}) - \xi J_1(\xi r_{sw})J_0(kr_{sw})}{\mu I_1(\mu r_{sw})J_0(\xi r_{sw}) + \xi J_1(\xi r_{sw})I_0(\mu r_{sw})} \right]. \quad (33)$$

In conclusion, having determined all the terms of the spectral density, we have arrived at an explicit form of (15):

$$\begin{aligned} \rho(\mathbf{k}, E) &= \frac{V_{sw}^2}{(E - k^2)^2(k^2 - \xi^2)^2} \left[ \frac{kJ_1(kr_{sw})J_0(\xi r_{sw}) - \xi J_1(\xi r_{sw})J_0(kr_{sw})}{\mu I_1(\mu r_{sw})J_0(\xi r_{sw}) + \xi J_1(\xi r_{sw})I_0(\mu r_{sw})} \right]^2 \\ &\quad \times \sum_i \delta(E - E_i(\mathbf{k}))[\lambda_i(k)\partial U/\partial E]^{-1}[\mathbf{u}_i \cdot \mathbf{e}]^2 \end{aligned} \quad (34)$$

where  $\lambda_i(k)U(E) = 1$  for  $E = E(k)$ . Here we also need to specify the band width,  $W$ , of electron states by using the scattering matrix,  $t_0(i\mu, i\mu)$  of the potential.

We would prefer to take, as far as possible, appropriate values for the atomic parameters, such as the strength of the potential and the bond length, even though we investigate the electronic structure of a model rather than a particular material. However, most published calculations use the tight-binding limit, which is only reached for real two-dimensional potentials by making them rather deep. Accordingly, in the following calculations we shall take the potential radius  $r = 0.5$  (au) and the bond length between two potentials  $R = 2.0$  (au), which results in a ground state energy of  $E_0 = -30$  (au). In this case, the atoms or ions are far apart from each other and so these assumptions lead to a very narrow band of allowed states around the atomic ground state energy,  $E_0$ . An alternative approach [15] for model calculations is to use a *delta-function-like* potential for which equation (33) becomes

$$\frac{s_0(k)}{s_0(i\mu)} = \frac{J_0(kr)}{I_0(\mu r)} \quad (35)$$

leading to a much simpler form for equation (34):

$$\rho(\mathbf{k}, E) = \frac{1}{(E - k^2)^2} \left[ \frac{J_0(kr)}{I_0(\mu r)} \right]^2 \sum \partial(E - E_i(\mathbf{k}))[\lambda_i(k)\partial U/\partial E]^{-1}[\mathbf{u}_i \cdot \mathbf{e}]^2. \quad (36)$$

As an initial illustration of the results, consider the limiting case of circular averaging. Equation (26) then gives one eigenvalue for each  $\mathbf{k}$ . The eigenvalues and the DOS are

plotted in figure 2. At the bottom of the band the DOS is free-electron-like, i.e., for two dimensions constant, nearer the bound state energy the DOS is dominated by a series of peaks which originate from the  $k$  values where  $\partial E/\partial k = 0$ . A slight broadening has been used in the figure to give a better qualitative indication of the structure of the DOS.

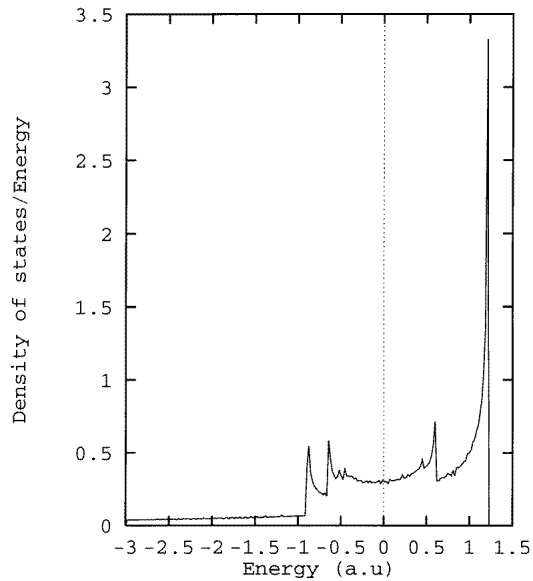


Figure 2. The DOS for the circularly symmetric average.

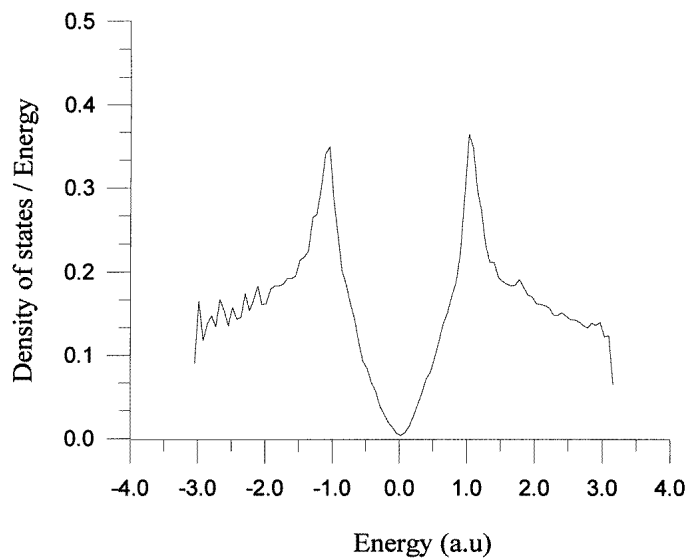
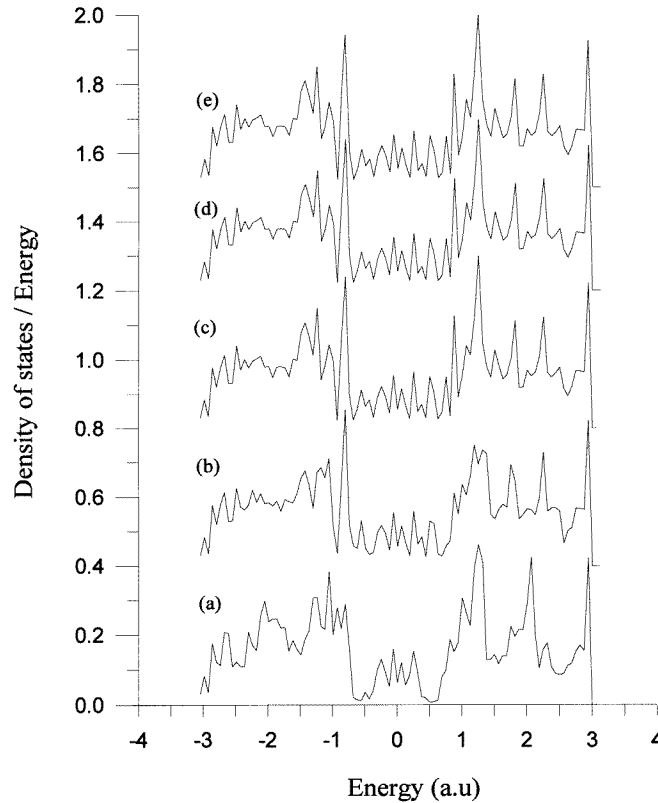


Figure 3. The DOS for a honeycomb perfect lattice model; disorder ( $\omega$ ) = 0.



**Figure 4.** The convergence of the DOS for disordered structures ( $\omega = 0.1$ ) with respect to the matrix sizes: (a)  $N \times N = 31 \times 31$ ; (b)  $N \times N = 51 \times 51$ ; (c)  $N \times N = 101 \times 101$ ; (d)  $N \times N = 301 \times 301$ ; (e)  $N \times N = 401 \times 401$ .

## 6. Results

In this section some illustrative results of the application of the procedure will be presented. Before considering the case of disorder, it is useful to confirm that the approach works for the perfectly ordered case, for which the theory should be equally correct. Accordingly, we have first calculated the perfect lattice case by taking the disorder parameter  $\omega = 0.0$ , to compare the curves to results which are expected and already well known. It can be seen in figure 3 that the DOS curves corresponding to a perfect honeycomb lattice structure agree well with the theoretical expectation (see, for example, [18]). Similar agreement is found for other lattice structures. The structure on this curve results from the size of the matrix used and would disappear if sufficient eigenvalues (i.e. sufficiently large matrices) were taken.

To investigate this convergence we have performed a series of calculations with increasing matrix size, in other words taking more eigenvalues and eigenvectors. This corresponds to using more accurate representations of the desired structure. In this analysis we have chosen a particular disorder value,  $\omega = 0.1$  (rad), for which we have evaluated the eigenvectors and eigenvalues for various sizes of the matrix. The smallest matrix used was  $31 \times 31$  and the largest  $401 \times 401$ . The results are presented in figure 4, again for

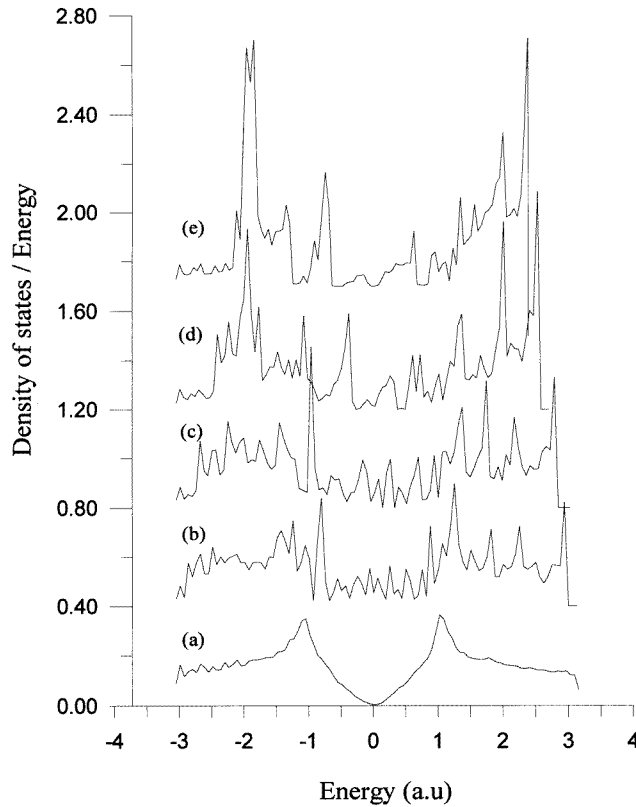


**Figure 5.** The DOS for honeycomb-lattice-like structural disorder ( $\omega$ ): (a)  $\omega = 0.0$ ; (b)  $\omega = 0.1$ ; (c)  $\omega = 0.2$ ; (d)  $\omega = 0.4$ ; (e)  $\omega = 0.7$ .

the honeycomb structure. It can be seen that there is little change beyond  $101 \times 101$  and no change beyond  $301 \times 301$ . This confirms an unproved expectation in BH that the method would converge; it was not possible to treat sufficiently large matrices to confirm this directly in the three-dimensional case.

The effect of varying disorder is shown in figure 5, using 301 eigenvalues. The top of the band is lowered in energy, as can be predicted from the wavefunctions for such states, which change sign between neighbouring atoms in the perfect lattice. This phase matching cannot be achieved in the disordered case. Similar arguments support the movement of states from the bottom of the band towards the bound state energy. A free-electron-like DOS of lower magnitude remains at the extreme bottom of the band. Some of the structure in these curves undoubtedly arises from the simplicity of the structural model used. Notice that even at large disorder the middle of the band is not significantly filled in.

A similar set of curves for four near neighbours is shown in figure 6. The same effects are seen at the bottom of the band and for large disorder the curve has a strong similarity to that for three near neighbours. Once the neighbouring atoms are spread uniformly around the central atom their number is little more than a multiplier on the bandwidth. For six near neighbours and large disorder the DOS is again similar. However, in this case the top of the band has risen in energy compared to the perfect lattice because it is easier to satisfy the phase changes between neighbours in the disordered than in the ordered case.

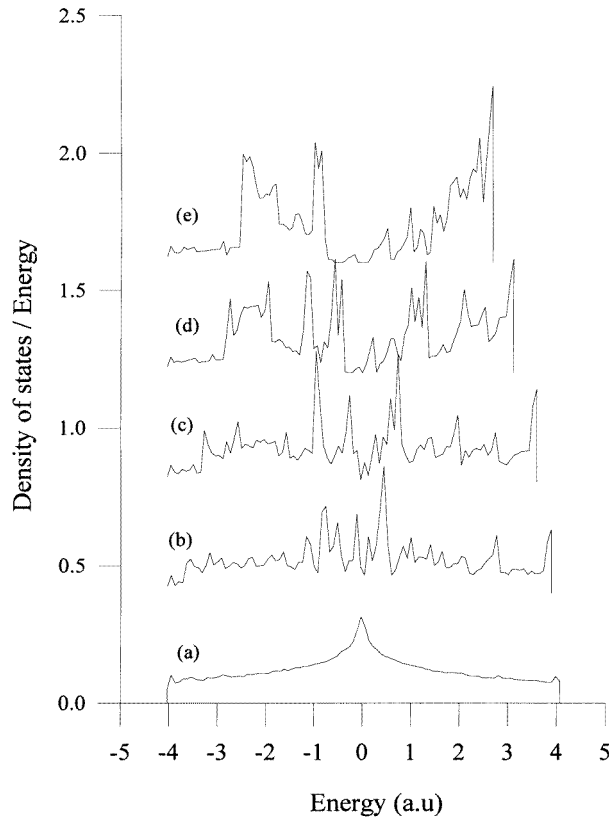


**Figure 6.** The DOS for square-lattice-like structural disorder ( $\omega$ ): (a)  $\omega = 0.0$ ; (b)  $\omega = 0.1$ ; (c)  $\omega = 0.2$ ; (d)  $\omega = 0.4$ ; (e)  $\omega = 0.7$ .

Finally, it is possible to perform the calculations for five near neighbours. The ordered case cannot exist so DOS calculated for that case is spurious, but at larger disorders the structures can be imagined and the DOS again resembles in shape that for three neighbours. The interesting case of quasicrystals has been discussed elsewhere using a variant of the method of this paper [15].

## 7. Discussion

The electronic structures of structurally disordered models in two dimensions have been investigated. The convergence of the technique as a function of matrix size has been demonstrated for a chosen disorder value ( $\omega = 0.1$ ). It was found that the DOS remained consistent above the matrix size of  $101 \times 101$  which was easily solvable and that a full calculation required a few a hours of workstation speed computer time.

The variation of the DOS with respect to the disorder parameter ( $\omega$ ) has been observed. Our results for these cases showed good agreement with theoretical expectation and so we have some evidence for the accuracy of our method. It was argued by Haydock [18] that a better approximation for perfect lattices makes the band edges sharper and improves the DOS in the bands. This has been observed in our calculations. On the other hand, in the

disordered cases it was found that the variation of the DOS significantly changed when the value of disorder ( $\omega$ ) exceeded 0.25 rad. As this value increased to 1.0 rad the weight in the DOS shifted towards the edges of the bands. We suspect that the shift may be related to the localization of electrons. However, for small disorder values ( $\omega \leq 0.25$ ) we have seen that the DOS spread towards the gap, and that the sharp edges were reduced in amplitude. It was argued by Choy [19] that the absence of odd-membered rings allows the DOS to be an even function of  $E$ , or the absence of even-membered rings allows the DOS to be an odd function of  $E$ . We have, in particular, investigated this argument and have concluded that our results are consistent with it, remembering that the structural disorder allows even-membered and odd-membered rings to coexist.

It would be possible to extend this study by going beyond nearest neighbours and introducing more structural information. However, it is not wholly realistic to assume that the number of neighbours stays constant as the disorder increases and a preferred extension of the approach is to allow the number of near neighbours to vary from atom to atom. Preliminary results suggest that such alloy-like calculations will be possible, allowing more progress towards realistic potentials in which electrons move in two-dimensional systems.

## References

- [1] van Rossum M C W and Nieuwenhuizen Th M 1994 *Phys. Rev. B* **49** 13 377
- [2] Rusek M and Orłowski A 1995 *Phys. Rev. E* **51** R2763
- [3] Ünal B and Alkan B 1995 *J. Phys.: Condens. Matter* **7** 3591
- [4] Fernandes de Mello D 1995 *Solid State Commun.* **94** 703
- [5] Kaveh M 1990 *Analogies in Optics and Microelectronics* ed W Van Haeringen and D Lenstra (Dordrecht: Kluwer) pp 21–34
- [6] van Albada M P, Lagendijk A and van der Mark M B 1990 *Analogies in Optics and Microelectronics* ed W Van Haeringen and D Lenstra (Dordrecht: Kluwer) pp 85–103
- [7] Schreiber and Ottemeier M 1992 *J. Phys.: Condens. Matter* **7** 1959
- [8] Dean P 1972 *Rev. Mod. Phys.* **44** 127
- [9] Elliot S R 1990 *Physics of Amorphous Materials* 2nd edn (New York: Longman–Wiley)
- [10] *Physics Through the 1990s: Condensed Matter Physics* 1986 (Washington: National Academy Press)
- [11] Stratford K 1993 *PhD Thesis* University of Leicester Department of Physics
- [12] Beeby J L and Hayes T M 1985 *Phys. Rev. B* **32** 6464 to be referred to as BH
- [13] Beeby J L and Hayes T M 1993 *Phys. Rev. B* **48** 17 732
- [14] Beeby J L and Hayes T M 1994 *Phys. Rev.* **B49** 14 128
- [15] Yildiz A K and Beeby J L 1996 *Phil. Mag.* **74** 387  
Yildiz A K 1995 *PhD Thesis* University of Leicester
- [16] Beeby J L 1964 *Proc. R. Soc. A* **267** 518
- [17] Abramowitz M and Stegun A (ed) 1965 *Handbook of Mathematical Functions: With Formulas, Graphs and Mathematical Tables* (New York: Dover) pp 361
- [18] Haydock R 1982 *Excitations in disordered systems* ed M F Thorpe (*ASI Series Physics B78*) (New York: Plenum) pp 43–57
- [19] Choy T C 1985 *Phys. Rev. Lett.* **55** 2915